PAPER

Theoretical insights into the sites and mechanisms for base catalyzed esterification and aldol condensation reactions over Cu†

Matthew Neurock,*[ab] Zhiyuan Tao,[b] Ashwin Chemburkar,[a] David D. Hibbitts[bc] and Enrique Iglesia[d]

Condensation and esterification are important catalytic routes in the conversion of polyols and oxygenates derived from biomass to fuels and chemical intermediates. Previous experimental studies show that alkanal, alkanol and hydrogen mixtures equilibrate over Cu/SiO_2 and form surface alkoxides and alkanals that subsequently promote condensation and esterification reactions. First-principle density functional theory (DFT) calculations were carried out herein to elucidate the elementary paths and the corresponding energetics for the interconversion of propanal + H_2 to propanol and the subsequent C−C and C−O bond formation paths involved in aldol condensation and esterification of these mixtures over model Cu surfaces. Propanal and hydrogen readily equilibrate with propanol *via* C−H and O−H addition steps to form surface propoxide intermediates and equilibrated propanal/propanol mixtures. Surface propoxides readily form *via* low energy paths involving a hydrogen addition to the electrophilic carbon center of the carbonyl of propanal or *via* a proton transfer from an adsorbed propanol to a vicinal propanal. The resulting propoxide withdraws electron density from the surface and behaves as a base catalyzing the activation of propanal and subsequent esterification and condensation reactions. These basic propoxides can readily abstract the acidic C_α−H of propanal to produce the $CH_3CH^{(-)}CH_2O*$ enolate, thus initiating aldol condensation. The enolate can subsequently react with a second adsorbed propanal to form a C−C bond and a β-alkoxide alkanal intermediate. The β-alkoxide alkanal can subsequently undergo facile hydride transfer to form the 2-formyl-3-pentanone intermediate that decarbonylates to give the 3-pentanone product. Cu is unique in that it rapidly catalyzes the decarbonylation of the C_{2n} intermediates to form C_{2n-1} 3-pentanone as the major product with very small yields of C_{2n} products. This is

[a]*Department of Chemical Engineering and Material Science, University of Minnesota, Minneapolis, MN, 55455, USA. E-mail: mneurock@umn.edu*

[b]*Department of Chemical Engineering, University of Virginia, Charlottesville, VA, 22904, USA*

[c]*Department of Chemical Engineering, University of Florida, Gainesville, FL, 32611, USA*

[d]*Department of Chemical and Biomolecular Engineering, University of California, Berkeley, CA 94720, USA*

likely due to the absence of Brønsted acid sites, present on metal oxide catalysts, that rapidly catalyze dehydration of the hemiacetal or hemiacetalate over decarbonylation. The basic surface propoxide that forms on Cu can also attack the carbonyl of a surface propanal to form propyl propionate. Theoretical results indicate that the rates for both aldol condensation and esterification are controlled by reactions between surface propoxide and propanal intermediates. In the condensation reaction, the alkoxide abstracts the weakly acidic hydrogen of the C_α−H of the adsorbed alkanal to form the surface enolate whereas in the esterification reaction the alkoxide nucleophilically attacks the carbonyl group of a vicinal bound alkanal. As both condensation and esterification involve reactions between the same two species in the rate-limiting step, they result in the same rate expression which is consistent with experimental results. The theoretical results indicate that the barriers between condensation and esterification are within 3 kJ mol^{-1} of one another with esterification being slightly more favored. Experimental results also report small differences in the activation barriers but suggest that condensation is slightly preferred.

1.   Introduction

Aldol condensation and Guerbet coupling as well as other alkanal/alkanol coupling reactions provide attractive routes for the removal of oxygen and hydrocarbon chain growth, which are important steps for the conversion of oxygenates to fuels as well as chemicals. Aldol condensation reactions are currently used industrially in the synthesis of 2-ethyl hexanal, methyl isobutyl ketone and Guerbet alcohols[2] and are also being considered for the conversion of bio-alcohols to fuels.[3,4] Aldol condensation and Guerbet reactions typically proceed *via* coupling of aldehydes and alcohols, respectively, to form β-hydroxy alkanals and alkanones that dehydrate to form α,β-unsaturated carbonyl intermediates on acid or base catalysts.[5] Base-catalyzed aldol condensation mechanisms are thought to proceed *via* the abstraction of the weakly acidic hydrogen at the α-C of an alkanal, thus resulting in the formation of an enolate that subsequently attacks the electrophilic carbonyl group of a vicinal alkanal to form a new C–C bond. These reactions can be carried out over a range of different homogeneous catalysts including Cu(II), Co(II), Mn(II), and Zn(II)[6] together with base promoters (NaOH, NaOR, and Na$_2$CO$_3$) or basic ligands,[7–10] as well as on heterogeneous base catalysts, including MgO,[11–14] Mg–AlO$_x$, ZnO,[15,16] phosphates,[17] and base-promoted mesoporous silicas, such as diamino-functionalized MCM-41 (ref. 18) and hydrotalcites.[19,20]

Previous kinetic studies have shown that while C_n alcohols react *via* aldol condensation paths to form C_{2n-1} alkanones over CuO/ZnO/Al$_2$O$_3$ and Cu/ZnO catalysts,[21] it is the basic sites on the ZnO support that are actually responsible for C–C bond formation. In a recent study, Sad *et al.*[1] demonstrated for the first time that both aldol condensation as well as esterification can proceed over non-basic catalysts, specifically monofunctional Cu/SiO$_2$ catalysts. Propanol (C$_3$H$_7$OH) was found to rapidly equilibrate with propanal (C$_3$H$_6$O) and H$_2$ to form an equilibrated propanol–propanal–H$_2$ reactant pool that subsequently reacts *via* the three predominant paths shown in Scheme 1: (1) dehydration of propanol to form propene and propane *via* subsequent hydrogenation steps; (2) aldol condensation followed by decarbonylation and dehydrogenation to form 3-pentanone (C$_5$H$_{10}$O)
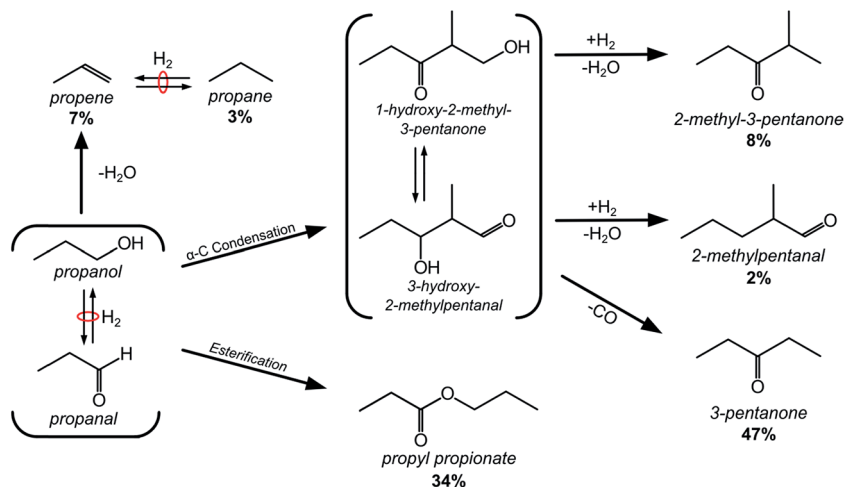
Scheme 1 Reaction paths for the conversion of propanol/propanal/H$_2$ over Cu/SiO$_2$, adapted from Sad et al.[1] Selectivities for six major products are given based on the following conditions: 5 wt% Cu/SiO$_2$, 5.6% dispersion, 503 K, 2160 g cat.-ks per mol propanol, 0.64 kPa propanol, 80 kPa H$_2$, balance He, 3% conversion.

or dehydration paths to form minor 2-methyl 3-pentanone and 2-methyl pentanal (C$_6$H$_{12}$O) products; and (3) esterification to form propyl propionate (C$_6$H$_{12}$O$_2$). The reported selectivities to form the propene, propane, 2-methyl-3-pentanone, 2-methyl pentanal, 3-pentanone, and propyl propionate at 3% conversion (shown in Scheme 1) are 7%, 3%, 8%, 2%, 47%, and 34%, respectively. Detailed kinetic analyses suggested that both esterification and condensation reactions proceed *via* the *in situ* formation of surface alkoxides on Cu that act as bases that catalyze C–C and C–O bond-forming reactions.

Further kinetic analyses showed that the rate equations for esterification and condensation follow the exact same functional form with the rate of condensation being ~2 times faster than the rate of esterification. This suggests that they proceed *via* a similar kinetically-relevant step that precedes a kinetic branch point unaffected by H$_2$ and alkanal/alkanol pressures, or that they have distinct kinetically-relevant steps that share the same reactant precursors.[1] Experimental results were used together with simple estimates from gas phase molecular calculations to suggest that condensation proceeds by the reaction of a surface enolate with an adsorbed propanal to form a hemi-acetalate (β-alkoxide alkanal) that decarbonylates to form 3-pentanone. In contrast, propyl propionate was proposed to be formed *via* a Cu-catalyzed esterification of two aldehydes, similar to the classic base-catalyzed esterification routes proposed by Cannizaro and Tishchenko as reported in the literature.[22,23]

First principle density functional theoretical (DFT) calculations were carried out herein to provide insights into the elementary steps, elucidate the mechanisms and establish the kinetics for Cu-catalyzed alcohol dehydrogenation, esterification and condensation. The simulation results indicate that propoxide surface intermediates are readily formed on Cu *via* the hydrogenation and dehydrogenation of the propanal and propanol, respectively, and act as a base,

co-catalyzing esterification and condensation pathways. Adsorbed alkanals can also catalyze promote hydride transfer from the adsorbed alkoxide intermediates to remove condensation and esterification products from the surface and to regenerate the catalytic propoxides.

2. Computational methods

All of the calculations reported herein were carried out using non-local gradient corrected periodic, plane-wave density functional theory (DFT) calculations using the Vienna *ab initio* Simulation Program (VASP).[24] The calculations were carried out over model Cu(111) surfaces to mimic the coordinatively-saturated sites that comprise >95% of the most active large Cu particles. The influence of edge and corner sites on the activation of C–H and O–H bonds of propanol were also examined by carrying out calculations on a Cu(110) surface and on a 201 atom cuboctahedral Cu cluster (Cu$_{201}$). The details for all of the simulations are reported in the ESI.†

The adsorption energies for all of the reactant, intermediate and product molecules were calculated as:

$$\Delta E_{ads} = E_{surf+ads} - E_{surf} - E_{ads} \tag{1}$$

where $E_{surf+ads}$, E_{surf}, and E_{ads} are the energies of the surface–adsorbate complex, the bare metal surface, and the adsorbate in vacuum, respectively. The activation barriers and reaction energies were calculated as:

$$A^* + B^* \rightarrow TS^* \rightarrow C^* + D^* \tag{2}$$

$$\Delta E_{act} = E_{TS^*} + \delta E_{surf} - E_{A^*} - E_{B^*} \tag{3}$$

$$\Delta E_{rxn} = E_{C^*} + E_{D^*} - E_{A^*} - E_{B^*} \tag{4}$$

where E_{i^*} and E_{TS^*} refer to the energies of adsorbed intermediate i (A*, B*, C* or D*) and the transition state (TS*), respectively. δE_{surf} refers to the change in energy required to bring the "infinitely" separated species on the surface together into the reactant state where they sit adjacent to one another, thus accounting for any attractive or repulsive interactions.

The intrinsic activation barriers for the elementary steps reported herein all refer to the direct energy difference between the transition state and the bound reactant(s) state along the elementary step reaction coordinate ($E_{TS^*} - E_{A^*} - E_{B^*}$ in eqn (3)). In order to compare with experimental results, we also calculate apparent activation energies where the transition state energies are referenced to the most abundant species present on the surface under reaction conditions rather than from the elementary step reactant state. Experimental results suggest that the surfaces are covered under reaction conditions. We therefore use adsorbed propoxide and the gas phase alkanal as the zero energy reference state to calculate apparent barriers for most of the systems discussed herein. The reaction entropies and free energies of activation were also calculated for the rate controlling esterification and condensation steps as discussed in ESI S.1.†

3. Results and discussion

3.1 Conversion between propanol and propanal

3.1.1 Equilibrium of propanal and hydrogen to propanol.

As was discussed earlier, mixtures of propanal and hydrogen along with propanol readily react and equilibrate over Cu/SiO_2. DFT calculations were used here to examine the elementary steps in the hydrogenation of propanal to propanol over Cu(111), as well at the reverse reactions for the dehydrogenation of propanol to propanal and hydrogen. Propanal was calculated to preferentially adsorb atop in an η_1 configuration resulting in an adsorption energy of -28 kJ mol^{-1} which is consistent with the adsorption site and energy reported from ultrahigh vacuum experimental studies carried out on Cu(111)[25,26] and previous theoretical studies[27–29] Hydrogen readily dissociates over the Cu(111) surface to form two H* surface species with an overall energy of -32 kJ mol^{-1}, consistent with experimentally reported adsorption energies of $\sim$40 kJ mol^{-1}.[30] The adsorbed propanal can subsequently hydrogenate by the initial addition of H* to the oxygen or the carbon of its carbonyl to form the hydroxypropyl (CH_3CH_2CH*OH) or propoxide (CH_3CH_2O*) intermediate, respectively, as shown in Scheme 2. The paths which proceed *via* propoxide and hydroxypropyl intermediates are known more generally in the literature as the alkoxide and hydroxyalkyl paths.

The propoxide path which is shown in Fig. 1 (unfilled symbols) proceeds by the initial addition of hydrogen to the carbon of the bound carbonyl to form the propoxide resulting in a barrier of 63 kJ mol^{-1} when taken with respect to the adsorbed propanal and a single H*, which mimics what would be measured on the covered surfaces found experimentally. The overall reaction energy for this step is highly exothermic with an overall energy of -52 kJ mol^{-1}. The propoxide intermediate subsequently hydrogenates to form adsorbed propanol. The intrinsic activation energy and the overall reaction energy to hydrogenate the propoxide to form propanol were calculated to be $+99$ kJ mol^{-1} and -21 kJ mol^{-1}, respectively. The propanol that forms desorbs from the surface with an energy of $+29$ kJ mol^{-1}. The overall potential energy surface for this path shown in Fig. 1 (unfilled symbols) suggests that propoxide forms and builds up on the surface as its rate of removal appears to be controlled by the high barrier for the second hydrogen addition step.

In the hydroxypropyl path which is shown in Fig. 1 (filled symbols), the barrier to add hydrogen first to the oxygen of the carbonyl rather than the carbon was
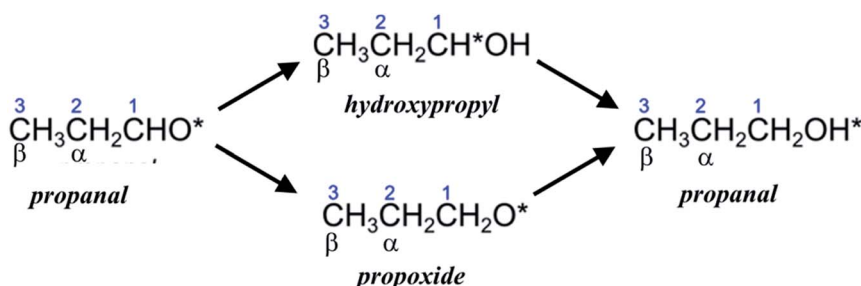
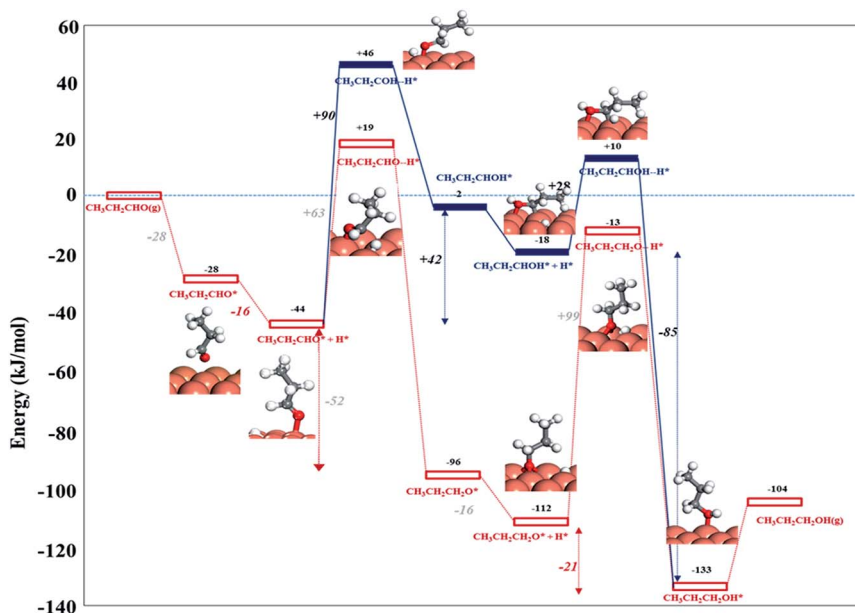**Scheme 2** Routes for the dehydrogenation of propanol to form propanal.

Fig. 1 DFT-calculated pathways for the hydrogenation of propanal to propanol and the reverse reaction involving the dehydrogenation of propanol to propanal and hydrogen. The propoxide path (unfilled rectangular symbols) involves the initial addition of hydrogen to the C_1 of the carbonyl to form the propoxide intermediate and the subsequent hydrogenation of the propoxide and the desorption of the propanol product. The hydroxypropyl path (filled rectangular symbols) proceeds instead by the initial addition of hydrogen to the O of the carbonyl to form the hydroxypropyl intermediate and the subsequent addition of hydrogen to the C of the hydroxypropyl to form propanol which desorbs.

calculated to be significantly higher at +90 kJ mol^{-1} taken with respect to the adsorbed propanal and H* as it requires the breaking of a strong Cu–O bond. The overall reaction energy to form the hydroxypropyl intermediates was calculated to be endothermic at +2 kJ mol^{-1}. The intrinsic activation barrier and overall reaction energy to subsequently hydrogenate the hydropropxyl intermediate to form adsorbed propanol were calculated to be 28 kJ mol^{-1} and −115 kJ mol^{-1} (taken with respect to the adsorbed hydropropxyl intermediate and H*), respectively. The results in Fig. 1 indicate that the rate for this path is likely limited by the initial hydrogen addition to the oxygen to form the hydroxyalkyl intermediate. A more detailed analysis of the energies for both the propoxide and the hydroxyalkyl paths shown in Fig. 1 suggests that the propoxide path is more favorable than the hydroxypropyl path, as the barrier to form the propoxide (+63) is 27 kJ mol^{-1} lower than that to form the hydroxypropyl (+90 kJ mol^{-1}). As such, the propoxide, regardless of the path, is readily formed and likely builds up on the surface and as a result is the kinetically dominant surface intermediate. This is consistent with previous analyses for the hydrogenation of different aldehydes and ketones over Ru.[31]

Propanol dehydrogenation, the microscopic reverse of propanal hydrogenation, is not likely to proceed over the Cu(111) surface as the intrinsic activation energies to activate the O–H or the C–H bond of propanol, taken with respect to

adsorbed propanol, are 115 and 143 kJ mol^{-1}, respectively, as is shown in Fig. 1. This is consistent with ultrahigh vacuum studies which show that, in the absence of oxygen, methanol as well as other light alcohols desorb and do not dissociate over Cu(111), and with other previous theoretical studies of methanol dehydration on Cu(111).[27,28] The results by Sad *et al.*[1] carried out over Cu/SiO$_2$ at higher pressures with mixtures of propanal, hydrogen and propanol, however, show that mixtures readily equilibrate. The difference in the reported reactivity of the alcohol on Cu are likely the result of higher propanol coverages at relevant reaction conditions which can assist O–H activation or *via* the presence and reactivity of coordinatively unsaturated sites that exist at edges or corners on the Cu particles. The results reported in Fig. S1† show that the barrier to activate the O–H bond of propanol decreases to 70 kJ mol^{-1} with increasing propanol surface coverage, as higher coverages result in the formation of hydrogen bonding networks which stabilize the transition state and allow facile proton-transfer *via* a Grotthus-like mechanism similar to that reported for other alcohol decomposition reactions in the presence of water over different metals.[32–34] While the higher coverages help to promote the formation of surface propoxide intermediates, the subsequent C–H activation would still likely be prohibitive as the barrier is 115 kJ mol^{-1} and does not decrease at higher coverages.

Propanol dehydration may proceed more favorably at the edge and corner sites of Cu particles. Both the O–H and C–H activation barriers decrease significantly to 73 kJ mol^{-1} when carried out at the more coordinatively unsaturated edge site on Cu(110) (Fig. S2†) which is consistent with experimental results for the activation of methanol, ethanol and propanol to form methoxy, ethoxy and propoxy, respectively, over Cu(110) under ultrahigh vacuum conditions.[35–38] We find similar low O–H and C–H activation barriers (<80 kJ mol^{-1}) for the dehydrogenation of propanol to propanal at the edge and corner sites on a Cu$_{201}$ cluster as presented in Fig. S3.† As such, propanol dehydrogenation to propanal and H$_2$ can occur at the edge and corner sites. The propanal and hydrogen that form can subsequently readsorb and react on the Cu(111) terrace sites to carry out condensation and esterification. This would still be consistent with the results from Sad *et al.*[1] which show that the rates increase with Cu particle size, thus indicating that the terrace sites are most active for the steps that control the rate.

3.2 Reactions of propanol and propanal

3.2.1 Base-catalyzed reactions on Cu. As discussed, esterification and aldol condensation reactions are thought to proceed over Cu *via* base-catalyzed reactions. The classic mechanism for a base catalyzed aldol condensation involves the base abstracting the weakly acidic proton from the C$_\alpha$–H bond of an alkanal or alkanone to form an enolate intermediate that subsequently attacks the electrophilic carbon on the carbonyl group of a vicinal alkanal or alkanone to form a β-hydroxy alkanal (aldol) as shown in Scheme 3A. The base can then dehydrate the aldol to form an α,β-unsaturated alkanal. Esterification proceeds *via* the nucleophilic attack of an alkoxide at the electrophilic carbon of the carbonyl group on the alkanal which then deprotonates to form an ester product, as shown in Scheme 3B.

While base-catalyzed aldol condensation and esterification reactions are well-established, neither Cu or SiO$_2$ exhibit basic sites; yet Cu/SiO$_2$ catalyzes both

A)

B)
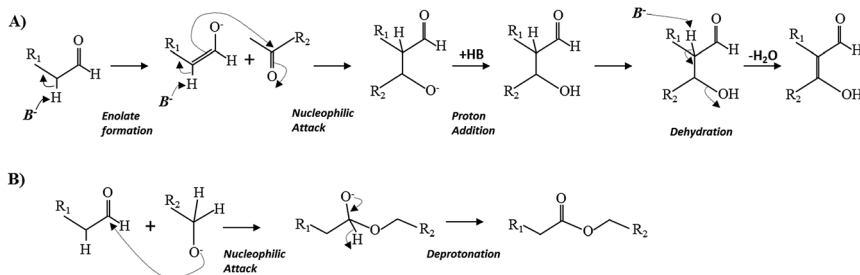
Scheme 3 Mechanism of base-catalyzed (A) aldol condensation and (B) esterification.

reactions.[1] The reaction instead has been proposed to proceed *via* the formation of a negatively-charged and basic propoxide intermediate on Cu, derived *in situ* from the interconversion of the equilibrated propanol–propanal–H_2 mixture. Alkoxides are electronically very similar to hydroxides which abstract electron density from group 11 metals to form weakly bound ($HO^{\delta-}*$) intermediates.[39–41] These weakly bound surface alkoxides can act as a base, thus enabling the activation of the weakly-acidic proton at the αC position of a vicinal aldehyde to initiate aldol condensation. In addition, the basic alkoxide intermediate can also nucleophilically attack the carbonyl of a vicinal alkanal to initiate esterification. Before describing the energetics of such reactions, we first present details on the electronic structure of these adsorbed alkoxide intermediates on transition metal surfaces.

3.2.2   Basic nature of RO* on Cu. Alkoxide anions (RO^-) in solution are bases that can readily abstract protons and carry out nucleophilic attack.[42] The properties and behavior of a bound alkoxide ($RO*$), on the other hand, is controlled by the electronic properties of the metal surface and the binding of the alkoxide to the metal, both of which are dictated by the direction and degree of charge transfer between the alkoxide and the metal. For noble metals such as Cu, Ag and Au, charge is transferred from the metal to the alkoxide. The charge transfer may be sufficient to allow for the formation of an anionic alkoxide intermediate, which would exhibit basicity comparable to solvated alkoxide anions. DFT-calculated electron densities for propoxide and propanal adsorbed at a 3-fold fcc site on Cu(111) are summarized in Table 1. Propoxide preferentially adsorbs to a three-fold fcc Cu site on the Cu(111) surface (Fig. 2a) with its C–O axis normal to the surface, resulting in a binding energy of -218 kJ mol^{-1}. The charge density

Table 1   Charge density differences on the oxygen of the alkoxide and alcohol before and after adsorption on the Cu(111) surface[a]

Species	Before adsorption (e^-)	After adsorption (e^-)
Cu_3[b]	0.13	0.71
O of $CH_3CH_2CH_2O*$	-0.33	-0.83
O of $CH_3CH_2CH_2OH*$	-0.62	-0.62

[a] The charge difference analysis is carried out using QUAMBO. [b] The total charge of the three Cu atoms of the 3-fold site.
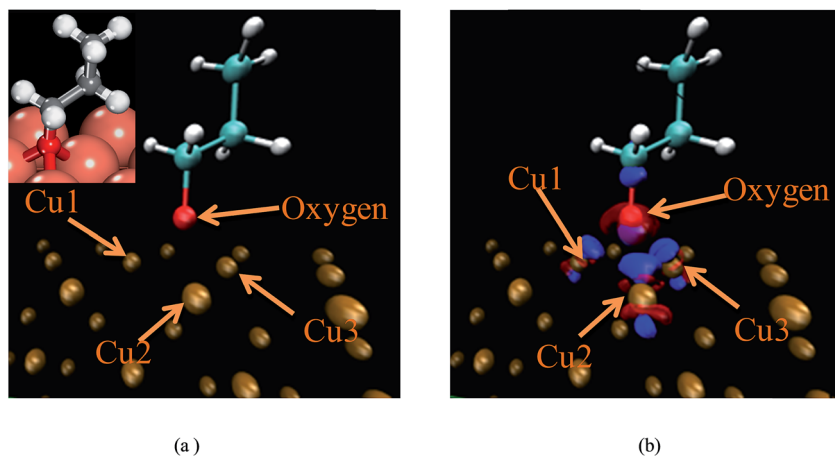
(a)   (b)

Fig. 2   (a) The adsorption structure for propoxide bound to a 3-fold fcc site on the Cu(111) surface; (b) charge density difference map between the adsorbed alkoxide and the alkoxide in the gas phase. The red isosurface depicts an increase of charge density whereas the blue isosurface reveals a decrease of charge density.

differences between the adsorbed and the separated propoxide/Cu system, depicted in Fig. 2b, show a significant shift in the electron density from the Cu to the oxygen upon adsorption. The results in Table 1 show a charge transfer of >0.5 e$^-$ from the Cu surface to the O-atom in the bound propoxide thus resulting in a negative -0.83 e$^-$ on the oxygen, which is consistent with anionic hydroxide and alkoxide species in solution, thus allowing it to behave as a base with properties similar to those of anionic alkoxides in solution. For comparison, we examined the charge transfer from the metal to the oxygen of molecularly adsorbed propanol. The results shown in Table 1 indicate that there is essentially no charge transfer from the metal to the propanol, as the charge on the O-atom following adsorption is less than 0.009 e$^-$.

The basicity of bound oxygen atoms and oxygen-containing intermediates on the group 11 (Cu, Ag, and Au) metals and other late transition metals including Pd, Pt, Rh and Ir has been discussed previously.[39–41,43–45] Hydroxide species (HO*) adsorbed to Au(111), Pt(111), or Pd(111) can readily abstract protons from water or from adsorbed alcohols during the dehydrogenation of alcohols to form aldehydes.[39–41] Adsorbed hydroxides (HO*) were also found to nucleophilically attack the carbonyl group at a vicinal alkanal to form the corresponding acid.[39–41] Herein, we examine the adsorption of the methoxide species as a simple probe alkoxide intermediate and compare the charges on the CH$_3$O* with those of OH*.

The charge transfer to the O of HO upon its adsorption to different 3d, 4d and 5d transition metals ranges from -0.77 e$^-$ on the more oxophilic metals (Pd, Rh and Ru) which bind O strongly, to -1.04 to -1.07 e$^-$ on the group 11 metals (Cu, Ag, Au) which bind O* weakly, as shown in Table S1 of the ESI.† Similarly, charge transfer from the metal to the O-atom in the adsorbed alkoxide (RO*) results in a charge on the oxygen that ranges from -0.54 on Rh and Ru to -0.83 e$^-$ on Cu, Ag, and Au. The results indicate that both RO* and HO* species on group 11 metal (Cu, Ag and Au) surfaces act as bases as they extract electron

density from the metal and become negatively charged (Table S1†). The charge transferred to the RO* and HO* species from other metals is significantly less than that from group 11 metals, likely due to the high electron density in the nearly-filled d-bands of these coinage metals (Cu: $3d^{10}$; Ag: $4d^{10}$; Au: $5d^{10}$).

3.2.3 C–H activation of propanal and propanol. Enolates, which are key intermediates in aldol condensation, form *via* the activation of the α-C–H bond of the aldehyde either by the metal surface or by an adsorbed alkoxide. $C_{2\alpha}$–H activation on Cu can proceed *via* an oxidative addition reaction where a Cu atom in the surface inserts into the C–H bond to form $CH_3CH^*CH=O$ and H* intermediates (eqn (5)).

$$CH_3CH_2CH_2OH^* \rightarrow CH_3CH^*CH_2OH + H^* \tag{5}$$

The weakly acidic $C_{2\alpha}$–H bond can also be activated by an adsorbed RO* intermediate which proceeds instead *via* proton abstraction by the alkoxide to form the corresponding alcohol and a surface enolate (eqn (6)).

$$CH_3CH_2CH_2OH^* + RO^* \rightarrow CH_3CH^*CH_2OH + ROH^* \tag{6}$$
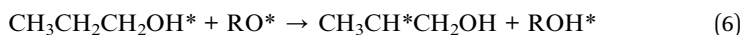
The α and β carbons of the propanol and propanal refer to the carbon atoms at the C_2 and C_3 positions, respectively, as is shown in Scheme 2. The barrier to activate the C_1–H bond of propanal *via* Cu-insertion to form the adsorbed CH_3-$CH_2C^*O^*$ acyl and H* intermediates is 91 kJ mol^{-1}, which is 10 kJ mol^{-1} lower than the barrier for Cu to activate the C_2–H bond of propanal to form surface $CH_3CH^*CHO^*$ and H* (101 kJ mol^{-1}) intermediates. While the C_2–H bond is weaker than the C_1–H bond, there are greater steric limitations in activating the secondary C_2–H bond than the primary C_1–H bond over metal surface sites. The steric constraints compensate for the C–H bond energies, thus resulting in a lower barrier to activate the primary C_1–H bond.

The activation of the $C_{2\alpha}$–H can also proceed in a heterolytic manner, through a reaction in which a vicinal propoxide ($CH_3CH_2CH_2O^{(\delta-)*}$) abstracts the weakly acidic α-H (with a charge of +0.166) to form propanol and an adsorbed enolate ($CH_3CH^{(-)*}CHO^*$). The barrier for the heterolytic activation of the $C_{2\alpha}$–H bond is 80 kJ mol^{-1} which is 21 kJ mol^{-1} lower than that for the homolytic $C_{2\alpha}$–H activation and 52 kJ mol^{-1} lower than that for the heterolytic activation of the C_1–H, as the C_1–H hydrogen is non-acidic (with a charge of +0.041). This is consistent with previous theoretical gas phase calculations, which show that the heterolytic abstraction of the C_1–H from the propanal *via* a gas phase OH intermediate is 60 kJ mol^{-1} higher than the abstraction of the acidic $C_{2\alpha}$–H of the propanal. The activation of the terminal C_3–H bond of propanal was found to be unfavorable on the Cu surface as well as by the vicinal bound propoxide. These results are consistent with calculated gas phase deprotonation energies and the charges on the H and C atoms of propanal and propanol (reported in Table 2) which provide a measure and ranking of their acidity. This is also consistent with pK_a values reported in the literature that show pK_a values for the $C_{2\alpha}$–H of different aldehydes range from 16–20, while those for the C_3–H hydrogen range from 40–50.[46]

The preferential activation at the $C_{2\alpha}$ site *via* basic surface species is consistent with experimental results[1] that show only the formation of 2-methyl-3-pentanone,

Paper

Table 2 DFT-calculated reaction and activation energies for the activation of C–H bonds in propanal and propanol together with the gas phase deprotonation energies of the bond that is broken as well as the charges on the H and C atoms on the C–H bond that is activated

C–H bond activation	Metal catalyzed		Alkoxide catalyzed				
	ΔE_{rxn}, kJ mol^{-1}	ΔE_{act}, kJ mol^{-1}	ΔE_{rxn}, kJ mol^{-1}	ΔE_{act}, kJ mol^{-1}	DPE, kJ mol^{-1}	Charge on CH H	Charge on CH C
C_1–H of propanal	41	91	24	122	1668	0.09	+0.45
$C_{2\alpha}$–H of propanal	52	101	34	70	1556	0.23	−0.50
C_3–H of propanal	112	166	91	162	1687	0.20	−0.59
C_1–H of propanol	118	144	107	166	1756	0.15	−0.02
C_2–H of propanol	117	166	104	155	1656	0.20	−0.41
C_3–H of propanol	129	174	117	163	1760	0.19	−0.58

2-methyl-3-pentanal and 3-pentanone products which form only *via* the reactions between a $C_{2\alpha}$ enolate and a vicinal bound propanal. The detailed elementary steps to form these products are reported in the next section. The formation of the linear 1-hexanal and 3-hexanone products which would form *via* the attack of $C_{3\beta}$ enolate on a vicinally bound propanal were notably absent.

The activation of each type of C–H bond in 1-propanol was also examined. The C_1–H bond is the most reactive on Cu as the –OH group withdraws electron-density from the C–H bonds at the terminal C-atom resulting in the following inductive effect: $CH_3^{(\delta+)} \rightarrow CH_2^{(\delta++)} \rightarrow CH_2^{(\delta+++)} \rightarrow OH^{(\delta-)}$.[46] A detailed charge analysis shows that the C_1 has a partial charge of −0.02 e$^-$, while C_2 has a partial charge of −0.41 e$^-$ and the C_3 has a partial charge of −0.58 e$^-$. As such, the barriers for C–H activation over Cu(111) at these three carbons increase from 144, 166 and 174 kJ mol^{-1} for C_1–H, C_2–H and C_3–H, respectively.

The barriers for activating the C_1–H and C_2–H bonds of propanol by the adsorbed alkoxide were calculated to be significantly higher than those for activating the C_1–H and C_2–H bonds of bound propanal. This is the result of the conjugation on the carbonyl that stabilizes the negative charge that results in abstracting a proton at the C_1 and C_2 position. Propanol, however, lacks the conjugation of the C=O bond and thus offers little stabilization of the negative charge. As such the C_1–H and C_2–H bonds of the alcohol are non-acidic. The barriers to activate the C_3–H bond for both propanol and propanal are very similar to one another as the –CH=O and –CH$_2$OH groups are now far enough removed from the C_3–H bond to influence its properties and reactivity.

The alkoxide chain length was varied to determine its effect on the barrier to activate the αC_2–H bond in propanal. The results shown in Table 3 indicate that hydroxides are slightly more basic than methoxides on Cu surfaces and thus are more effective in the activation of the mildly acidic αC_2–H bond. This is likely due to the fact that the O-atom in OH* is more negative than the O in CH$_3$O* and thus more basic. For larger alkoxides, the activation barriers increase slightly with chain length, from 65 kJ mol^{-1} for methoxide to 72 and 70 kJ mol^{-1} for ethoxide and propoxide, respectively. These small increases are the result in steric hindrance between the alkoxide and aldehyde on the surface and will likely disappear with the inclusion of dispersion.

Table 3 Reaction and activation energies for the αC_2–H bond activation of propanal with different RO* species on Cu(111)

$C_{2\alpha}$–H bond activation	ΔE_{rxn}, kJ mol^{-1}	ΔE_{act}, kJ mol^{-1}
Metal catalyzed	52	101
HO* (R = H)	35	56
CH$_3$O* (R = CH$_3$)	36	65
CH$_3$CH$_2$O* (R = CH$_3$CH$_2$)	34	72
CH$_3$CH$_2$CH$_2$O* (R = CH$_2$CH$_2$CH$_3$)	30	70

The theoretical analyses reported here show that C–H bond activation in propanal preferentially proceeds *via* proton-transfer to RO* bound to the Cu surface. The RO* species acts as a base and abstracts the most acidic hydrogen, which is located at the α-C-atom in propanal, to form enolate species that can subsequently react with a second adsorbed alkanal *via* aldol condensation to form a new C–C bond. The barriers to activate the C$_1$–H (99 kJ mol^{-1}) and C$_3$–H (166 kJ mol^{-1}) bonds in the aldehydes and the C$_1$–H (144 kJ mol^{-1}), C$_2$–H (166 kJ mol^{-1}) and C$_3$–H (174 kJ mol^{-1}) bonds in the alcohols with the bound propoxide were all significantly higher than the base-catalyzed activation of the C$_{2\alpha}$–H, as all of the other hydrogens are non-acidic and as such will not be activated by a base.

3.3 Aldol condensation paths on Cu

Base-catalyzed aldol condensation of two C_n alkanals typically proceeds through the activation of the first alkanal to form an enolate. The enolate subsequently attacks the carbonyl in the vicinal-bound alkanal to form a β-alkoxy-alkanal intermediate that rapidly protonates to form the C_{2n} β-hydroxy alkanal (aldol) as shown in the first step in Scheme 4. The aldol can readily dehydrate to form an α,β-unsaturated alkanal (a conjugated enone). In the propanal reactions examined here, the C_{2n} aldol (3-hydroxy-2-methyl-pentanal) dehydrates to form 2-methyl-2-pentenal (α,β-unsaturated alkanal), that can readily hydrogenate resulting in the observed 2-methyl-2-pentanal product, as shown in the upper
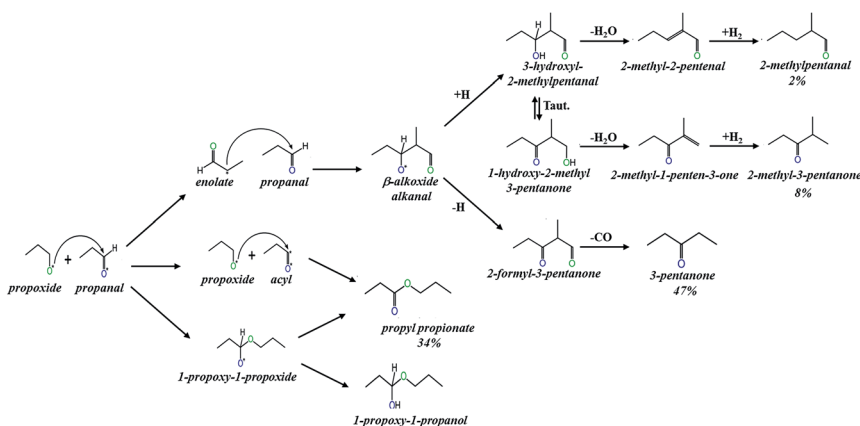
Scheme 4 Possible reaction pathways following aldol condensation.

branch in Scheme 4. The 2-methyl-2-pentanal product, however, only accounts for 2% of the products observed and neither the aldol (3-hydroxyl-2-methylpentanal) or the conjugated enone (2-methyl-2-pentenal) products were observed experimentally.[1] As such, this path is only a minor route for condensation. The second condensation product observed, 2-methyl-3-pentanone (8% selectivity) forms *via* tautomerization or intra-molecular hydrogen transfer reactions that convert the aldol (3-hydroxy-2-methylpentanal) to the β-hydroxy ketone (1-hydroxy-2-methyl-3-pentanone) which subsequently dehydrates and then hydrogenates to form 2-methyl 3-pentanone that desorbs from the surface.[1] This is the path in the center of Scheme 4.

The predominant condensation product is 3-pentanone which makes up ∼82.5% of all of the condensation products formed and ∼47% of the total products which include those from esterification as well as direct dehydration. The prevalence of the 3-pentanone product is consistent with previous studies that indicate that the most favorable coupling products are C_{2n-1} ketones.[47,48] This suggests that aldol condensation is followed by rapid decarbonylation or decarboxylation where oxygen is removed as either CO or CO_2. These decarbonylation/decarboxylation reactions can proceed *via* an intra or inter (*via* reactions with a vicinal alkanal) molecular hydrogen transfer to form the β-diketo intermediate (2-formyl-3-pentanone). The β-diketo can subsequently react *via* a retro-aldol reaction to eliminate CO and form 3-pentanone (shown as the lower condensation path in Scheme 4).

The first step in aldol condensation, which involves the propoxide-catalyzed activation of the weakly acidic C_α–H bond of propanal to form the enolate, was calculated to have an intrinsic activation barrier of 70 kJ mol^{-1} (taken with respect to the adsorbed propoxide and propanal) (Fig. 3A and Table 2). The enolate subsequently reacts with a vicinal bound alkanal to form the β-alkoxide alkanal surface intermediate with a barrier of only 19 kJ mol^{-1} and an overall reaction energy of −26 kJ mol^{-1} (Fig. 3B). The structures of the reactant, transition and product states for all of the initial aldol condensation steps are shown in Fig. 3.

3.3.1 Formation of 2-methyl-2-pentanal. The β-alkoxy-alkanal (β-alkoxy-2-methyl pentanal) intermediate formed *via* the C_3-enolate attack on the propanal can hydrogenate to give the 3-hydroxy-2-methyl-pentenal which subsequently dehydrate and then hydrogenate to form the 2-methyl-2-pentanal product shown in the upper path in Scheme 4. This sequence proceeds by the protonation of the β-alkoxide alkanal as shown in Fig. 3C and has an intrinsic activation barrier of 69 kJ mol^{-1} calculated with respect to the adsorbed β-alkoxide and H*. While the subsequent dehydration and hydrogenation steps to form the minor 2-methyl-2-pentenal product readily proceed, they were not examined herein. The tautomerization and subsequent dehydration and hydrogenation of the 1-hydroxy-2-methyl 3-pentanone to form the 2-methyl-3-pentanone product (center condensation path in Scheme 4) were also not examined.

3.3.2 Formation of 3-pentanone. The predominant aldol product as discussed above is 3-pentanone, which proceeds *via* dehydrogenation of the β-alkoxide alkanal and its subsequent decarbonylation (bottom condensation path in Scheme 4). The C–H activation of the β-alkoxide alkanal over Cu (Fig. 3D) was calculated to be prohibitive with an intrinsic barrier of 105 kJ mol^{-1}.
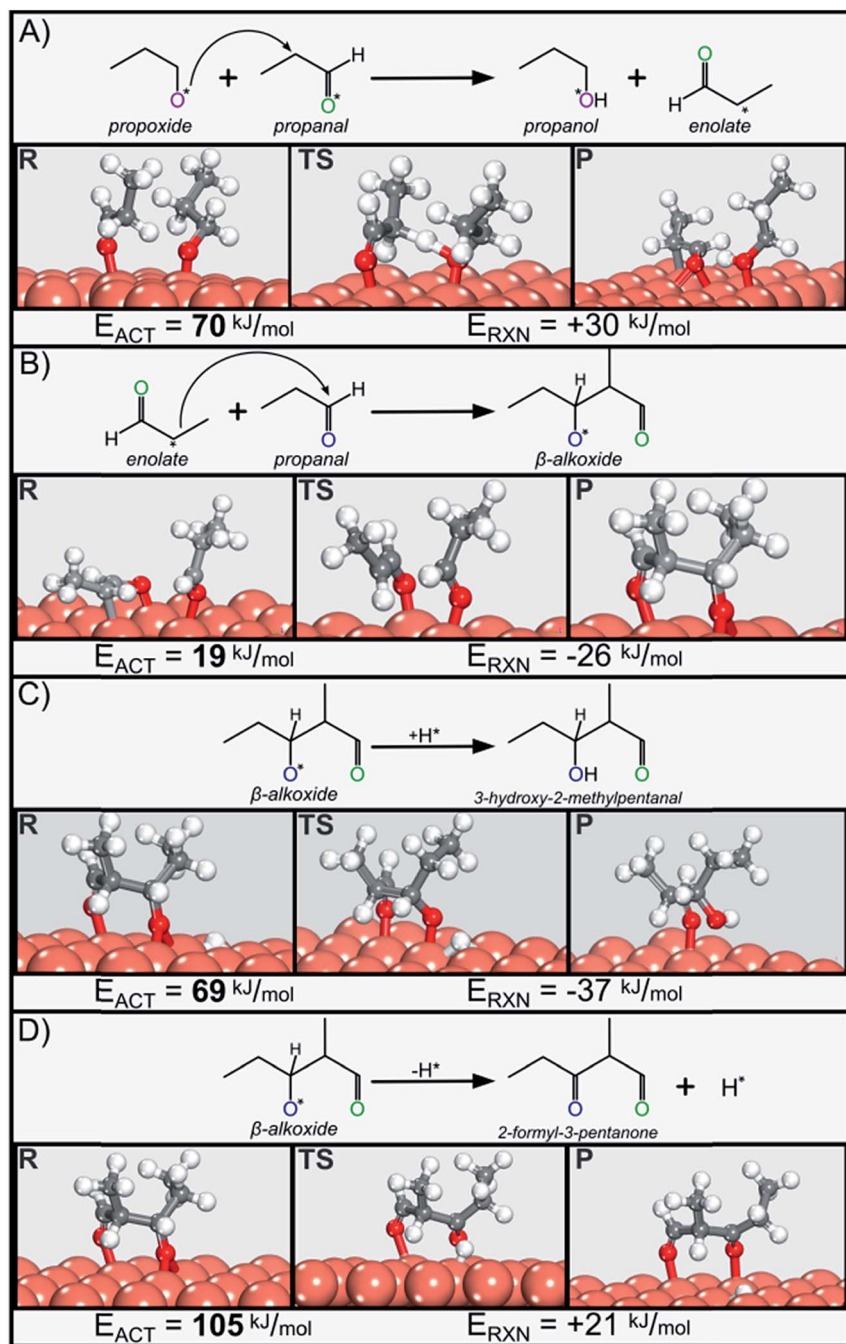
Fig. 3 DFT-calculated reactant, transition and product states along with the intrinsic activation barriers and the overall reaction energies for elementary steps in the aldol condensation of adsorbed propoxide and propanal over Cu(111) to form the 3-hydroxy-2-methylpentanal and 2-formyl-3-pentanone intermediates. These include: (A) activation of the weakly acidic $C_{2\alpha}$–H of propanal by a surface propoxide to form a surface enolate, (B) enolate attack on the C=O bond of a vicinal propanal to form β-alkoxide alkanal, (C) protonation of the β-alkoxide alkanal to form the aldol, and (D) C–H activation of β-alkoxide alkanal to form 2-formyl-3-pentanone.

The reaction instead appears to proceed *via* intermolecular hydrogen transfer. The C_1–H hydrogen of the alkoxide is hydridic in character, and as such, it can be readily abstracted by a vicinal-bound electrophile such as the bound propanal. The barrier to activate the C_1–H bond of the β-alkoxide alkanal by a coadsorbed propanal was calculated to be 74 kJ mol^{-1} (ΔE_{rxn} = 0 kJ mol^{-1}), as shown in Fig. 4A. The intrinsic barrier for the propanal activation of the β-alkoxide alkanal to form 2-formyl-3-pentanone is 31 kJ mol^{-1} lower than that calculated for the Cu C_1–H activation (105 kJ mol^{-1}). The adsorbed Cu–O=CHR adduct behaves as a Lewis acid that assists H-transfer.

The surface enone (2-formyl-3-pentanone) can subsequently decarbonylate *via* a direct retro-aldol CO elimination from the C_1-alkoxide alkanal intermediate as shown in Scheme 4. The barrier for this path, however, was calculated to be >110 kJ mol^{-1}. Decarbonylation can instead proceed *via* the initial activation of the C_1–H bond of the 2-formyl-3-pentanone intermediate to form the surface 2-acyl-3-pentanone ($CH_3CH_2C(O)CH(CH_3)CO^*$) intermediate with an intrinsic activation barrier of +74 kJ mol^{-1} and an overall reaction energy of +42 kJ mol^{-1} (see Fig. 4B). This C_1–H activation subsequently weakens the C_1–C_2 bond thus allowing for direct C=C bond scission over Cu to form 3-pentene-2-olate ($CH_3CH_2C(O^*)CHCH_3$) and CO* products with an intrinsic activation energy of only +7 kJ mol^{-1} and an overall reaction energy of −40 kJ mol^{-1} (Fig. 4C). The resulting 3-pentene-2-olate ($CH_3CH_2C(O^*)CHCH_3$) intermediate subsequently hydrogenates to form 3-pentanone with a barrier of +68 kJ mol^{-1} and a reaction energy of −60 kJ mol^{-1} (Fig. 4D) which then desorbs from the surface.

The final aldol condensation path considered is rather different than the first two paths in that it proceeds *via* the initial C–H activation of the alkanal to form an acyl (RCO*) intermediate, that subsequently attacks a vicinal bound propanal to form the aldol product directly.[27] This path was found to be unlikely as the intrinsic activation barriers for the initial C–H activation and subsequent C–C bond formation steps were calculated to be very high at 133 and 153 kJ mol^{-1}, respectively.

The activation barriers and reaction energies for the elementary steps presented in Fig. 3 and 4 above were used to construct overall reaction energy diagrams for different pathways, determine rate expressions for each path and establish the lowest energy route. The results are presented in detail in ESI S.4.† In all paths, we assume that propanal and hydrogen are equilibrated with propanol (see Section 3.2). For simplicity, all of the paths are therefore referenced to the same adsorbed propanal and propoxide initial state, defined as $E = 0$.

The lowest energy paths which are shown in Fig. 5 proceed *via* the coupling of propoxide and propanal surface intermediates to form the 2-methyl-pentanal and 2-methyl-3-pentanone products. The condensation rates are ultimately dictated by the barrier to form the enolate (70 kJ mol^{-1}) *via* the abstraction of the weakly acidic $C_{2\alpha}$–H hydrogen by a vicinal propoxide, which is the highest point along the overall energy path taken with respect to adsorbed propanal and propoxide, the most abundant surface intermediates.

The enolate can readily attack the carbonyl of a vicinal propanal to form the β-hydroxide alkanal that subsequently reacts by: (1) H* addition to form the aldol that then reacts to form 2-methyl-pentanal and 2-methyl-3-pentanone products,
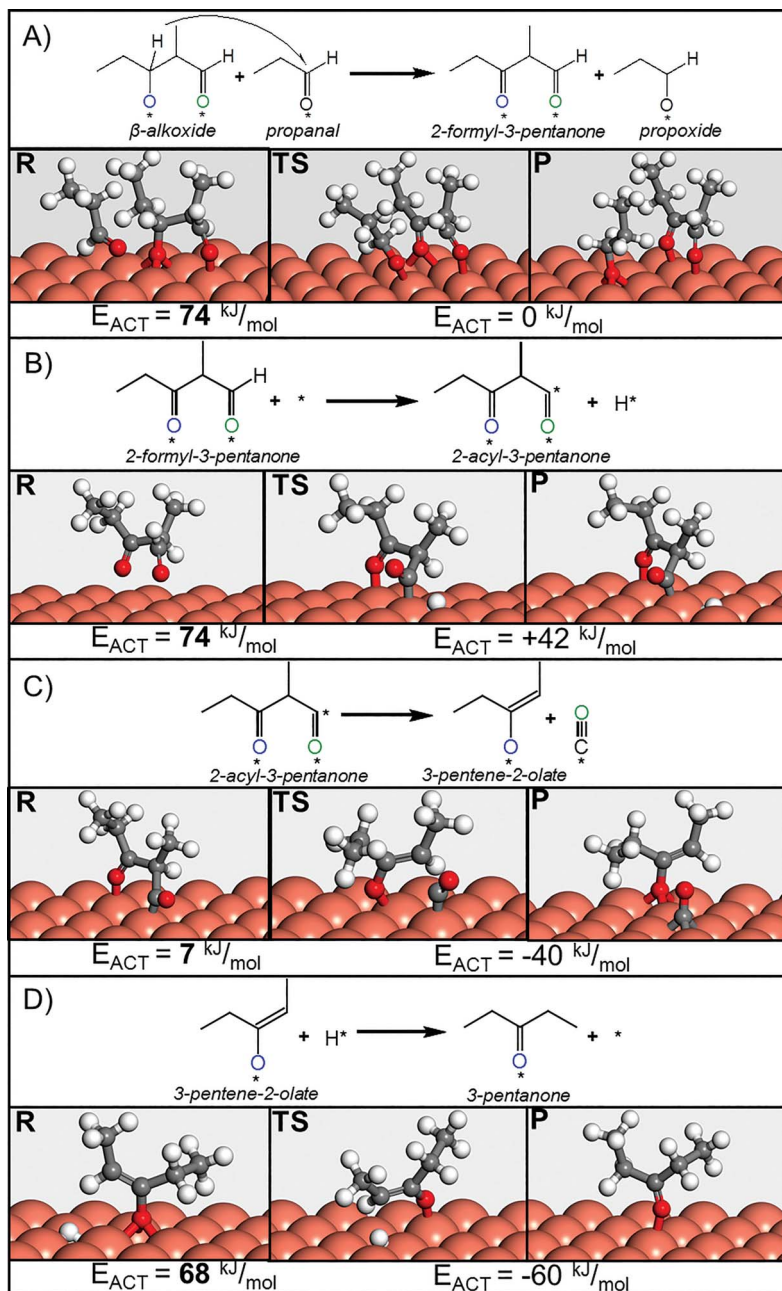
Fig. 4 DFT-calculated reactant, transition and product states along with the intrinsic activation barriers and the overall reaction energies for elementary steps in the conversion of the dehydrogenated aldol intermediate, β-alkoxy-2-methyl pentanal, to 3-pentanone over Cu(111). The steps include: (A) intermolecular hydride transfer from β-alkoxide alkanal to adsorbed propanal to form the 2-formyl-3-pentanone intermediate, (B) C_1−H scission of the 2-formyl-3-pentanone to form 2-acyl-3-pentanone, (C) decarbonylation of 2-acyl-3-pentanone to form 3-pentene-2-olate and CO and (D) hydrogenation of 3-pentene-2-olate to form 3-pentanone.
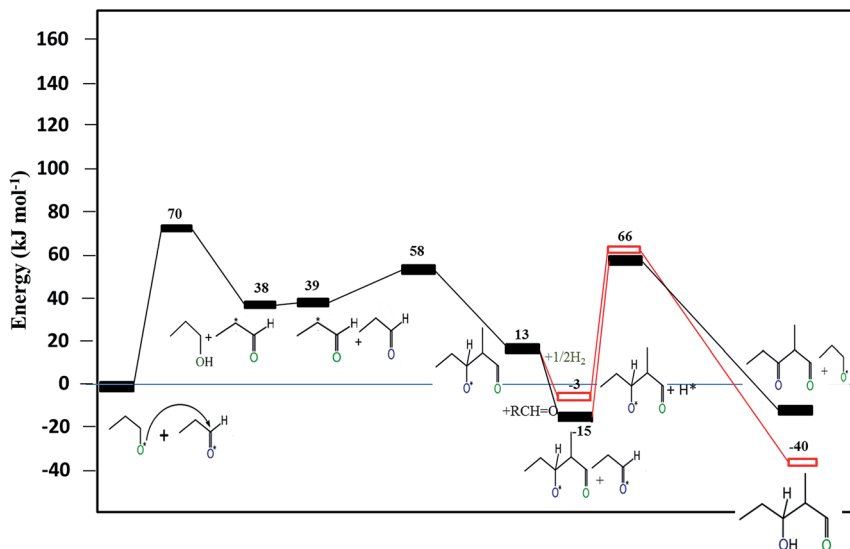
Fig. 5   The lowest energy DFT-calculated pathways for the aldol condensation reactions of propanol–propanal on Cu(111) proceed *via* the coupling of the enolate and propanal to form the β-alkoxide alkanal which can: (i) hydrogenate (shown with unfilled rectangular symbols) to form the aldol or (ii) dehydrogenate *via* hydride transfer from an adsorbed propanal to form 2-formyl-3-pentanone (shown with filled rectangular symbols).

or (2) hydride abstraction by a vicinal propanal to form a 2-formyl-3-pentanone intermediate which subsequently undergoes C–H activation and decarbonylates over Cu to form 3-pentanone (Fig. 6).
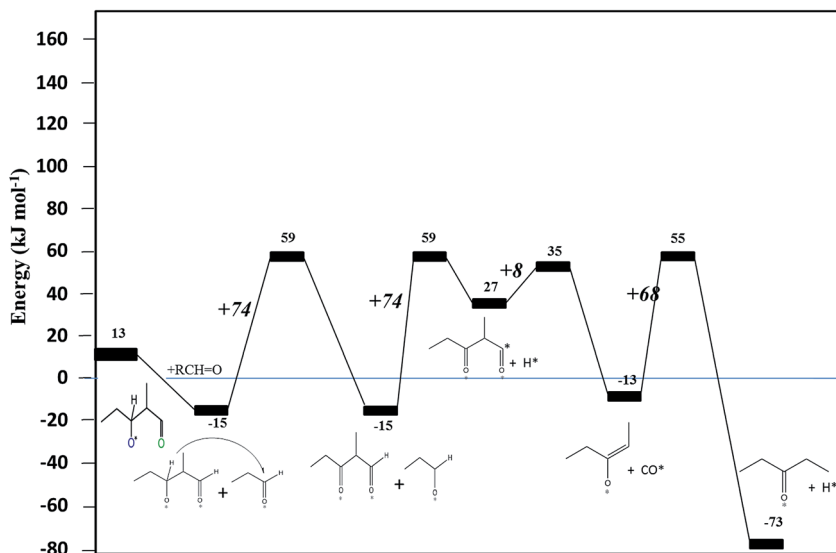

Fig. 6   DFT-computed pathways for the decarbonylation of the 1-propoxy-1-propoxide intermediate to form 3-pentanone on Cu(111). Activation barriers for each step are shown in larger font and in italic.

The rate for both propoxide and propanal coupling reactions is controlled by the initial activation of the weakly acidic $C_{2\alpha}$–H bond on the alkanal by a basic propoxide surface intermediate and can be written as:

$$r_{cond} = k_{cond}[\text{propanal*}][\text{propoxide*}]$$
$$= k_{cond}K_{PAL}{}^2K_{HYD_1}K_{H_2}{}^{1/2}P_{PAL}{}^2P_{H_2}{}^{1/2}/[1 + K_{PAL}P_{PAL}$$
$$+ K_{PAL}K_{HYD}K_{H_2}{}^{1/2}P_{PAL}P_{H_2}{}^{1/2}]^2$$

(7)

where k_{cond} refers to the intrinsic rate constant for deprotonation of the weakly acidic $C_{2\alpha}$–H bond; K_{PAL}, K_{HYD_1}, and K_{H_2} are the equilibrium constants for the adsorption of propanal, the hydrogenation of propanal to the surface propoxide over Cu and the dissociative adsorption of hydrogen, respectively, and P_{PAL} and P_{H_2} refer to the partial pressure of propanal and hydrogen, respectively. The apparent activation barrier for this path calculated with respect to the adsorbed propanal and propoxide is simply the 70 kJ mol^{-1} barrier for the initial $C_{2\alpha}$–H activation by the propoxide to form the enolate (Fig. 3A). The theoretical results suggest that propanal and propoxide are the abundant surface intermediates. Experimentally-measured rates of reaction as a function of the pressures of propanal and hydrogen indicate that while both propanal and propoxide exist on the surface, the propanal is the most abundant surface intermediate.[1]

3.4 Esterification paths on Cu

Base-catalyzed esterification reactions typically proceed *via* Tischenko-type pathways involving the reaction between an adsorbed alcohol and aldehyde. Three potential paths by which the surface alkoxide and alkanal species can react over Cu are shown in Scheme 5. The first path (E$_1$ in Scheme 5) proceeds *via* nucleophilic addition of the surface alkoxide to the vicinal alkanal to form
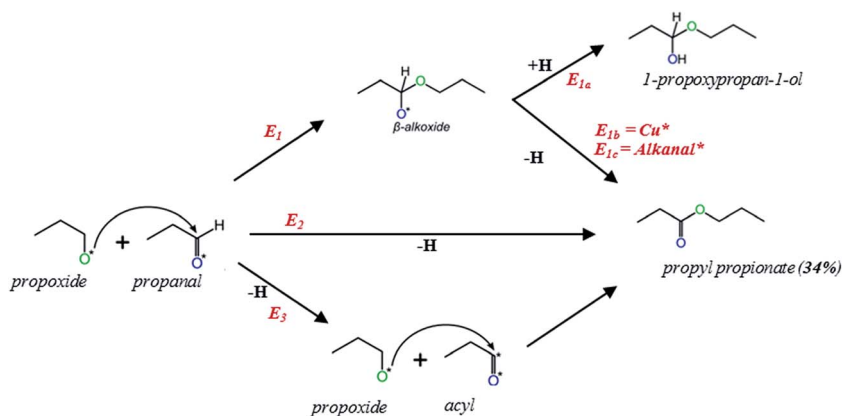
Scheme 5 Three possible reaction paths for the esterification paths involving C–O bond formation *via* the coupling of propanal and propoxide intermediates over Cu. E$_1$ paths proceed by sequential C–O formation followed by hydrogen addition (E$_{1a}$) or hydrogen elimination *via* Cu (E$_{1b}$) or *via* an adsorbed alkanal (E$_{1c}$). The E$_2$ path follows simultaneous C–O formation and H-elimination. E$_3$ proceeds *via* the initial activation of the propoxide to form an acyl intermediate.

a hemiacetalate (1-propoxy-1-propoxide) surface intermediate. The reaction proceeds by an initial shift of the alkoxide from its stable 3-fold adsorption site to a bridging site where it readily attacks the carbonyl C of the neighboring propanal intermediate to form the C–O bond, resulting in an intrinsic barrier of 60 kJ mol^{-1}. A significant portion of the activation barrier is associated with the incipient activation of the strong Cu–OC$_3$H$_7$ bond to form the more weakly bound and reactive propoxide. The Cu–OC$_3$H$_7$ weakening is compensated by the formation of a strong Cu–OCH(OCH$_2$CH$_2$CH$_3$)(CH$_2$CH$_3$) bond in the resulting 1-propoxy-1-propoxide intermediate, as shown in Fig. 7A. The 1-propoxy-1-propoxide can subsequently dehydrogenate either by Cu-catalyzed C$_1$–H bond cleavage to form the propyl propionate product and a surface H* (path E$_{1b}$ in Scheme 5) or *via* intermolecular hydride transfer from the C$_1$–H bond of the 1-propyl-1-propoxide to a vicinal propanal species (E$_{1c}$) thus resulting in the formation of propyl propionate and a surface propoxide. The Cu-catalyzed C$_1$–H activation of the hemiacetalate (1-propoxy-1-propoxide) was found to be rather difficult with a barrier of 90 kJ mol^{-1} (as shown in Fig. 7B) which is nearly identical to the barrier for propoxide C$_1$–H activation (91 kJ mol^{-1}) reported in Table 2. The propanal-catalyzed hydride transfer occurs *via* a Meerwein–Ponndorf–Verley (MPV) type mechanism as shown in Fig. 7C resulting in a barrier of only 31 kJ mol^{-1}, which is 59 kJ mol^{-1} lower than the barrier to activate the C$_1$–H bond over Cu. The lower barrier for propanal-catalyzed hydride transfer compared to that for Cu-catalyzed C–H activation is consistent with the results for the propanal- and Cu-catalyzed C$_1$–H activation of the β-alkoxide alkanal discussed in Section 3.3 for aldol condensation. The hydride-transfer barrier from the 1-propyl-propoxide in the esterification reaction, however, is 43 kJ mol^{-1} lower than that from the β-alkoxide alkanal in the condensation path, as the oxygen in the ester significantly increases the hydricity of the C$_1$–H bond by stabilizing the charge in the transition state.

In addition to dehydrogenation, the 1-propoxy-1-propoxide can also hydrogenate *via* protonation of the alkoxide to form the 1-propoxy-1-propanol hemiacetal (path E$_{1a}$ in Scheme 5) resulting in a barrier of 104 kJ mol^{-1} (Fig. 7D). The 1-propoxy-1-propanol can desorb from the surface or dehydrogenate to form a propyl propionate product.

The surface propoxide and propanal can also react together in a second path (path E$_2$ shown in Scheme 5) that proceeds *via* a concerted S$_N$2 type reaction involving the nucleophilic attack of the surface propoxide on the carbonyl of the surface propanal (C–O bond formation) together with the simultaneous elimination of C$_1$ propoxyl hydrogen to the Cu surface to form propyl propionate directly. The transition state for this concerted path (Fig. 7E) involves the elongation of the C–O and C=O bonds in the ester (1.39 Å and 1.28 Å, respectively) relative to their product state (1.34 Å and 1.24 Å), which helps to assist the activation of the propoxyl C$_1$–H bond. The intrinsic barrier for this reaction taken with respect to the adsorbed propanal and propoxide was calculated to be 69 kJ mol^{-1} (Fig. 7E), which is slightly higher than that for the direct coupling of surface propanal and propoxide, thus making it a viable path for esterification and the direct formation of propyl propionate.

The third and final path to form propyl propionate is characteristically different than the first two paths in that it proceeds by initially activating the C$_1$–H bond of the alkanal to form an acyl intermediate. The acyl subsequently reacts
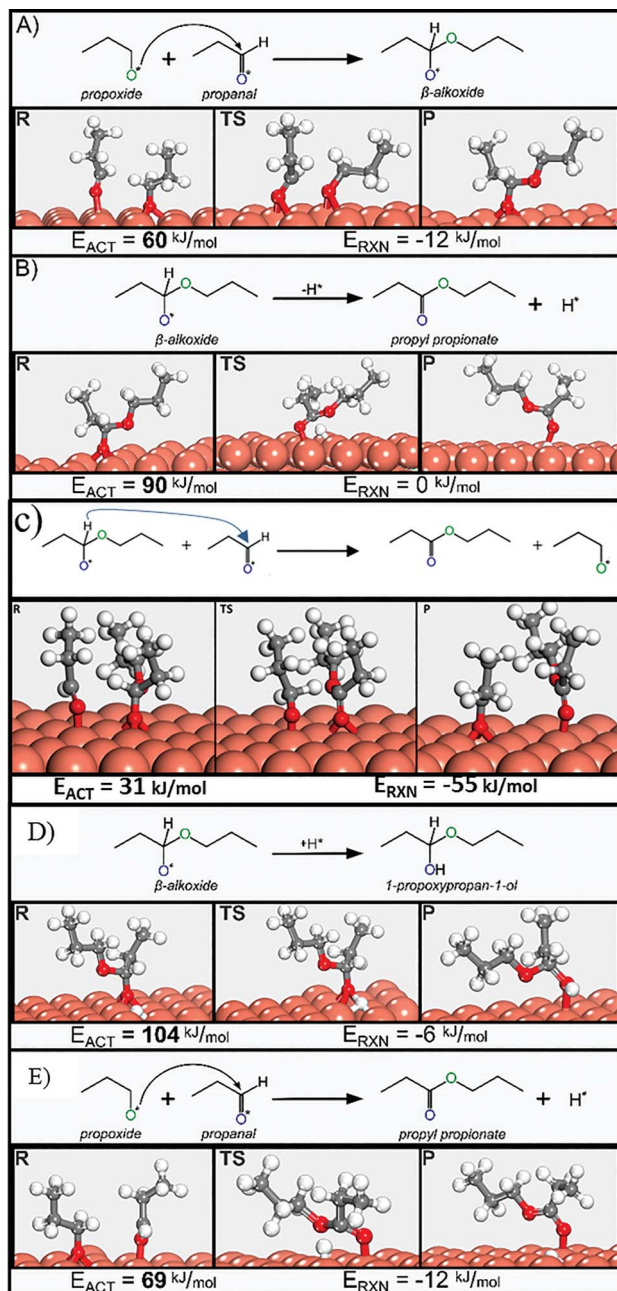
Fig. 7 DFT-calculated reactant, transition state and product state structures and the corresponding activation barriers and overall reaction energies for different elementary steps in the esterification of propanal and propanol over Cu(111) surface to form propyl propionate. The steps include: (A) the nucleophilic attack of the adsorbed propoxide on the adsorbed propanal (C−O bond formation), (B) C_1−H activation by a surface Cu site, (C) intermolecular hydride transfer from the C_1−H of the 1-propoxy-1-propoxide intermediate to a vicinal bound propanal, (D) hydrogenation of the 1-propoxy-1-propoxide to form the 1-propoxy-1-propanol hemiacetal, and (E) concerted S_N2-type nucleophilic attack of the adsorbed propoxide on the adsorbed propanal and C_1−H hydrogen elimination to Cu.

with a surface alkoxide to form the ester product directly (path E_3 in Scheme 5).[1] The intrinsic barrier to activate the alkanal to form the surface acyl intermediate is rather high at 101 kJ mol^{-1}. The acyl subsequently couples with a co-adsorbed propoxide with an intrinsic barrier of 81 kJ mol^{-1}, which is significantly higher than the coupling barrier between propanal and propoxide (53 kJ mol^{-1}). This does not appear to be a viable path to the esterification products that form.

The elementary steps and corresponding activation and reaction energies for the different esterification paths presented above are discussed in detail in ESI S.5.† The lowest energy routes in Table 1 were used to construct the two viable energy paths presented in Fig. 8 and the operative kinetic expressions for esterification. For simplicity, the paths presented in Fig. 8 are referenced to adsorbed propanal and propoxide as these species rapidly equilibrate, as was discussed in Section 3.2.

Both paths presented in Scheme 5 (and in Fig. 8) proceed *via* reactions involving surface bound propoxide and propanal intermediates, as shown in paths E_{1c} and E_2. These paths are similar in nature to those reported previously for methanol[49,50] and ethanol[51] esterification over Au. The results in Fig. 8 indicate that both paths proceed in a very similar manner *via* the coupling of the surface propoxide and propanal in the rate controlling step. The E_{1c} path involves sequential C–O formation and H-transfer steps whereas E_2 proceeds *via* simultaneous C–O formation and H-transfer to form the hemiacetal directly.
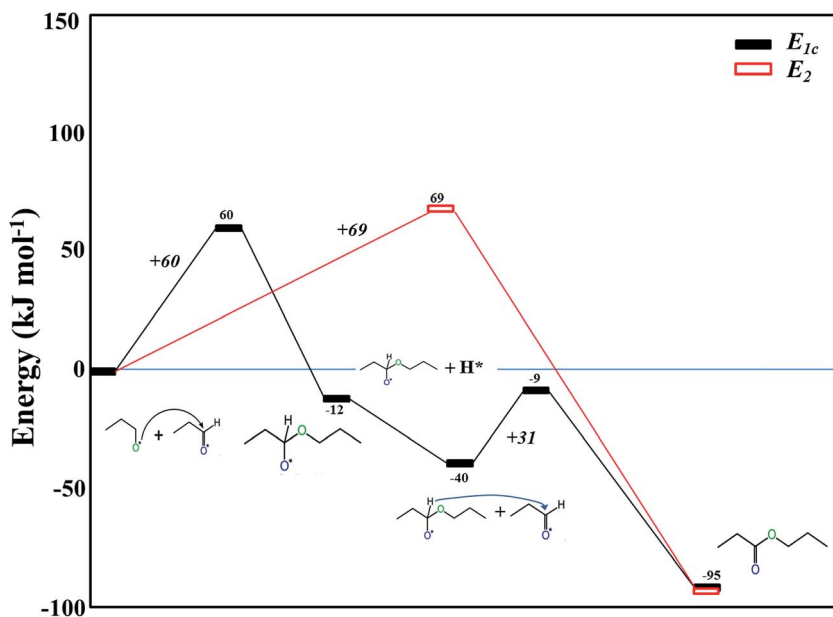

Fig. 8 DFT-calculated reaction paths for the esterification of propanol–propanal on Cu(111). The E_{1c} path (filled rectangular symbols) proceeds *via* the coupling of a surface alkoxide and surface alkanal to form the β-alkoxide hemiacetalate species which subsequently reacts with a second vicinal propanal to eliminate H to form the propyl propionate. The E_2 path (unfilled rectangular symbols) proceeds *via* a concerted coupling of the surface propyl and propanal intermediates together with the C_1–H activation by Cu.

The rate equations for these paths are identical and can be written as:

$$r_E = k_E[\text{propanal*}][\text{propoxide*}]$$
$$= k_E K_{PAL}^2 K_{HYD_1} K_{H_2}^{1/2} P_{PAL}^2 P_{H_2}^{1/2} /$$
$$[1 + K_{PAL} P_{PAL} + K_{PAL} K_{HYD_1} K_{H_2}^{1/2} P_{PAL} P_{H_2}^{1/2}]^2 \tag{8}$$

where k_E is the intrinsic rate constant for the coupling of surface propoxide and propanal for paths E_{1c} and E_2; K_{PAL}, K_{HYD_1} and K_{H_2} are the equilibrium constants for the adsorption of propanal, hydrogenation of adsorbed propanal to the adsorbed propoxide, and the dissociative adsorption of hydrogen, respectively, and P_{PAL} and P_{H_2} refer to the pressure of propanal and hydrogen, respectively.

Experimental results indicate that the propanal is the most abundant surface intermediate. As such the rate expression in eqn (8) would reduce to reduce to:

$$r_E = k_E K_{HYD_1} K_{H_2}^{1/2} P_{H_2}^{1/2} \tag{9}$$

The equilibrium constants for the surface and gas phase hydrogenation of propanal to propanal, $K_{H_2}^{1/2}$ and K_{HYD_1}, are directly included in the E_{1c} and E_2 barriers as they were measured with respect to the propanal and propoxide directly. The apparent activation barriers for the E_{1c}, and E_2 paths were therefore calculated to be 60 and 69 mol^{-1}, respectively and as such, both are viable paths for esterification.

The results reported here indicate that the ester is formed either by an E_{1c} path which involves a sequential mechanism where the rate-controlling C–O formation step, involving the coupling of a surface propoxide and propanal, precedes a rapid hydride transfer from the alkoxide C–H bond to the vicinal bound propanal or by an E_2 path which proceeds *via* the concerted coupling of a surface propoxide with coadsorbed propanal and direct hydrogen elimination to the surface. Both of these paths result in rate expressions and propanal and hydrogen dependencies that match those reported experimentally.[1]

3.5 Comparing free energies for condensation and esterification

In order to appropriately compare the rates of condensation and esterification we calculated the enthalpies, entropies and the free energies for the most favorable condensation and esterification paths. The activation energies reported earlier for condensation (70 kJ mol^{-1}) and esterification (60 kJ mol^{-1} for the E_{1c} and 69 kJ mol^{-1} for the E_2 paths) were calculated at 0 K. These values were subsequently corrected for zero point energies as well as changes that result in specific heats in moving from 0 to 298 K. The resulting activation enthalpies at 298 K for condensation (66 kJ mol^{-1}) and esterification (60 kJ mol^{-1}) were used together with the activation entropies reported in Table 4 to determine free energy barriers of 69 kJ mol^{-1} and 66 kJ mol^{-1} for the condensation and esterification reactions, respectively. The difference between the condensation and esterification free energy barriers is only 3 kJ mol^{-1} with the esterification being slightly favored.

Sad *et al.*[1] showed that rates of esterification and condensation follow identical dependencies on the partial pressures of propanal as well as propanol and hydrogen, as is shown in Fig. S5 in the ESI.† The ratio of the rate of condensation to the rate of esterification was found to be constant over a range of propanal

Table 4 Comparison of the activation enthalpies, entropies and free energies for the condensation and esterification of propanal and propoxide species on the Cu(111) surface

	Condensation	Esterification
$\Delta H^{\neq}$ (kJ mol^{-1})	66	60
$\Delta S^{\neq}$ (kJ (mol K)$^{-1}$)	−0.009	−0.013
$\Delta G^{\neq}$ (kJ mol^{-1})	69	66

pressures as well as propanol and hydrogen pressures as is shown in Fig. S5.† This suggests that rates of condensation and esterification obey similar rate equations but contain different rate constants,[1] indicating that their respective kinetically-relevant steps involve the same adsorbed propanal (CH$_3$CH$_2$CHO*) and surface propoxide (CH$_3$CH$_2$CH$_2$O*) intermediates. The two steps are limited by kineti-cally-relevant propoxide–propanal reactions mediated by bimolecular transition states, but lead to different products. This is fully consistent with the theoretical results discussed above and summarized in Fig. 9 that show that the rate-controlling step for condensation involves the abstraction of the weakly acidic H at the α-position of propanal by basic propoxide to form the enolate intermediate whereas that for esterification involves nucleophilic addition of the basic prop-oxide to bound propanal.

In condensation, the enolate species that forms in the rate-limiting step can readily attack a vicinal propanal to form a β-alkoxide alkanal which can undergo facile inter- or intra-molecular hydride transfer to form the aldol species that can subsequently dehydrogenate and decarbonylate to form 3-pentanone (shown in the upper path in Fig. 9). The 1-propoxy-1-propoxide intermediate that forms in the rate controlling step for esterification can undergo facile intermolecular hydride transfer to a surface propanal (path E$_{1c}$
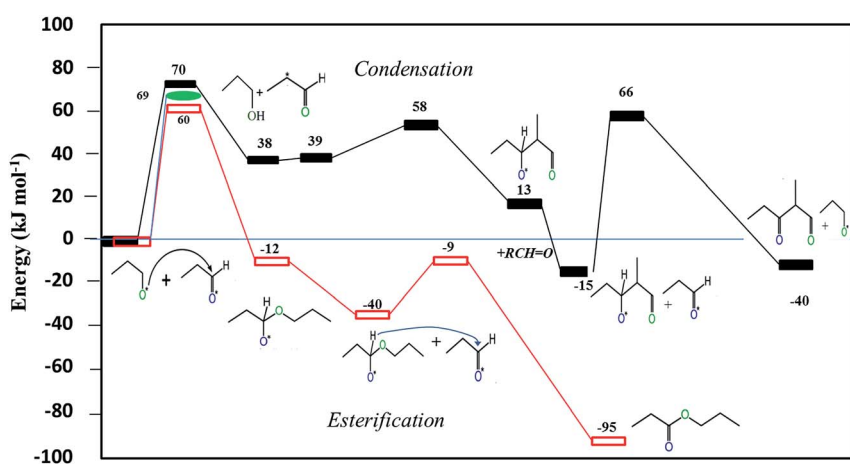

Fig. 9 A comparison between the energies for the elementary steps involved in aldol condensation and esterification reactions over Cu. The aldol condensation is shown in the top curve, denoted by dark filled rectangular symbols. Esterification can proceed either via the E$_{1c}$ path involving sequential C–O formation and intermolecular hydride transfer which is shown in the unfilled rectangular symbols or via the E$_2$ concerted C–O formation H-elimination path shown in the green elliptical symbols.

which is the lower path in Fig. 9) or a concerted S_N2-like mechanism (path E_2 shown with filled oval symbol) involving simultaneous C–O formation *via* the coupling of the surface propoxide with coadsorbed propanal and direct H-elimination to form the propyl propionate product.

The ratio of the rates shown in Fig. S5† can be analyzed by writing out the ratio of the rate expressions for condensation (eqn (7)) to esterification (eqn (8)). This ratio simplifies to a ratio of rate constants for C–C bond formation (k_C) *versus* C–O bond formation (k_E):

$$\frac{r_C}{r_E} = \frac{k_C}{k_E} = \frac{A_C \exp(-E_{aC}/RT)}{A_E \exp(-E_{aE}/RT)} = \frac{A_C}{A_E} \exp(-(E_{aC} - E_{aE})/RT) \qquad (10)$$

where r_C, r_E, E_{aC}, E_{aE}, A_C, and A_E are the rates, activation energies and pre-exponential factors respectively and the subscripts C and E denote condensation and esterification routes.

The experimental rate data reported by Sad *et al.* (shown in Fig. S4†) indicate that condensation rates are about two-times larger than those for esterification at all pressures at 503 K.[43] This corresponds to an esterification barrier that is ~3 kJ mol^{-1} higher than that for condensation (*i.e.* $E_{aC} - E_{aE} = -3$ kJ mol^{-1}), provided that both reactions have similar pre-exponential factors. Theoretical treatments (Fig. 9) show that the barriers for aldol condensation and esterification are similar, with a condensation barrier that is 3 kJ mol^{-1} higher than that for esterification ($E_a^{Cond} - E_a^{Est} = 3$ kJ mol^{-1}). Although the sign is different between experimental and theoretical estimations, the difference between these two is well within the accuracy of density functional theory of ± 5 kJ mol^{-1}.[52]

Previous experimental results show that Cu can uniquely catalyze condensation as well as esterification reactions. Such reactions are typically catalyzed by acids and bases for reactions that are carried out over metal oxides. The theoretical and experimental results presented here show that the exposed Cu metal surface sites act as Lewis acid sites that readily bind the oxygen of alkanal, alkanol and alkoxide intermediates and work cooperatively with basic sites formed *via* the *in situ* generation of propoxide intermediates to create acid–base site pairs that can rapidly equilibrate alkanal/hydrogen/alkanol mixtures and catalyze condensation and esterification reactions.

Alkoxy intermediates on Cu as well as other group 11 metals (Au and Ag) are more weakly bound to the metal than those on other transition metal surfaces as a result of significant Pauli repulsion with the nearly filled d-band of Cu and other group 11 metals. They act to abstract electron density from the metal, thus creating negatively charged alkoxides that behave as a base and work together with the Lewis acid sites to form acid–base site pairs that can readily activate acidic C–H and O–H bonds and carry out nucleophilic attack.

The nearly filled nature of the d-band of Cu, as well as other group 11 metals, limits their ability to readily activate C–H bonds alone. The Cu surface atoms, however, can act as Lewis acid sites and bind to the O of the alkanal thus creating an enol-like surface intermediate that can undergo electrophilic additions, readily accept hydridic H atoms and catalyze the activation of C–H bonds. These adsorbed alkanals are electron acceptors and thus behave as weak Lewis acids. They work closely with the basic alkoxide sites of the surface to provide acid–base site pairs, similar to those on metal oxides such as TiO$_2$,[53,54] and ZrO$_2$ (ref. 55–57) that can readily catalyze aldol condensation and esterification reactions. The

cooperative influence of weak Lewis acid–base pairs for these reactions and others was pioneered by Tanabe.[58,59] Cu is unique in that it selectively carries out decarbonylation along with C–C bond formation. This is likely due to the fact that Cu does not form Brønsted acid sites upon the deprotonation of C–H or O–H bonds but instead delivers the proton to weakly held alkoxide intermediates to produce non-acidic alcohols. The Brønsted acid sites that form metal oxide catalysts, on the other hand, readily promote hemiacetal formation and in addition catalyze dehydration reactions which lead to the hemiacetal and deoxygenated alkanal and alcohol products.

4. Conclusions

First principles density functional theory calculations demonstrate that Cu can catalyze both aldol condensation and esterification reactions without the addition of basic oxide promoters or a basic oxide support. This chemistry is facilitated by the *in situ* production of adsorbed alkoxide species which act as a base as well as an active nucleophile, effectively replacing the role of the basic oxide support. In addition, the adsorbed alkanal species weakly bind to Cu to form enolic-type Lewis acid sites that catalyze the activation of hydridic C_1–H bonds for various different reactive intermediates. Propanal, propanol and H_2 readily react to form an equilibrated mixture that subsequently undergoes aldol condensation and esterification reactions. The primary product from aldol condensation is 3-pentanone which is formed *via* C–C coupling followed by decarbonylation. 2-methyl-pentanal and 2-methyl-3-pentanone, which are the predominant products over typical acid and base catalysts as a result of subsequent dehydration steps, are only produced in minor amounts (<10%), indicating that decarbonylation is facile on these Cu/SiO_2 catalysts. Cu was also found to catalyze the C–O bond formation for the reactions between propanol and surface propionate, resulting in the formation of propyl propionate as a second primary product.

The alkoxide that forms from the interconversion of propanal + H_2 and propanol mixtures withdraws electron density from the Cu substrate, thus resulting in the formation of an alkoxide anion that behaves as a base that catalyzes both aldol condensation and esterification. The alkoxide can directly abstract the acidic α-H of aldehyde to form the C_3 enolate during aldol condensation and can carry out the nucleophilic attack of the carbonyl of the adsorbed aldehyde to form C–O bonds during esterification. These two steps have the highest activation barriers and appear to be the kinetically-relevant steps for the condensation or esterification paths, respectively. Since the kinetically-relevant steps for both the condensation and esterification reactions proceed *via* identical reactants (*i.e.* propanal and propoxide), both reactions result in the same rate equations and have identical kinetic dependencies on the partial pressures of propanal and hydrogen which is consistent with the experimental results. The calculated difference in the activation barriers for rate-limiting steps for esterification (C–O bond formation) and condensation (enolate formation) is small at 3 kJ mol^{-1}. This is consistent with the small differences in the activation barriers found experimentally, but condensation is favored experimentally over esterification.

Acknowledgements

References

1 M. E. Sad, M. Neurock and E. Iglesia, *J. Am. Chem. Soc.*, 2011, **133**, 20384.

2 C. A. Hamilton, S. D. Jackson and G. J. Kelly, *Appl. Catal., A*, 2004, **263**, 63.

3 J. N. Chheda and J. A. Dumesic, *Catal. Today*, 2007, **123**, 59.

4 R. M. West, Z. Y. Liu, M. Peter, C. A. Gartner and J. A. Dumesic, *J. Mol. Catal. A: Chem.*, 2008, **296**, 18.

5 T. Lowry and K. S. Richardson, *Mechanism and Theory in Organic Chemistry*, Harper and Row, NY, 1987.

6 H. Henschela, M. H. Prosencb and I. A. Nichollsa, *J. Mol. Catal. A: Chem.*, 2011, **351**, 76.

7 N. Kumagai, S. Matsunaga, N. Yoshikawa, T. Ohshima and M. Shibasaki, *Org. Lett.*, 2001, **3**, 10.

8 N. Kumagai, S. Matsunaga, T. Kinoshita, S. Harada, S. Okada, S. Sakamoto, K. Yamaguchi and M. Shibasaki, *J. Am. Chem. Soc.*, 2003, **125**, 2169.

9 R. Mahrwald and B. Ziemer, *Tetrahedron Lett.*, 2002, **43**, 4459.

10 H. Inoue, M. Kikuchi, J. Ito and H. Nishiyama, *Tetrahedron*, 2008, **64**, 493.

11 J. I. Di Cosimo, V. K. Diez and C. R. Apesteguia, *Appl. Catal., A*, 1996, **137**, 149.

12 G. Wang, Z. Zhang and Y. W. Dong, *Org. Process Res. Dev.*, 2003, **8**, 18.

13 Y. Shigemasa, K. Yokoyama, H. Sashiwa and H. Saimoto, *Tetrahedron Lett.*, 1994, **3**, 1263.

14 Z. Zhang, Y. W. Dong and G. W. Wang, *Chem. Lett.*, 2003, **32**, 966.

15 C. A. Hamilton, S. D. Jackson and G. J. Kelly, *Appl. Catal., A*, 2004, **263**, 63.

16 A. E. Palomares, G. Eder-Mirth and J. A. Lercher, *J. Catal.*, 1998, **180**, 56.

17 R. Zeng, X. Fu, C. Gong, Y. Sui, X. Ma and X. Yang, *J. Mol. Catal. A: Chem.*, 2005, **229**, 1.

18 B. M. Choudary, M. L. Kantam, P. Sreekanth, T. Bandopadhyay, F. Figueras and A. Tuel, *J. Mol. Catal. A: Chem.*, 1999, **142**, 361.

19 J. C. A. A. Roelofs, D. J. Lensveld, A. J. Dillen and K. P. de Jong, *J. Catal.*, 2001, **203**, 184.

20 M. J. Climent, A. Corma, S. Iborra and A. Velty, *J. Catal.*, 2004, **221**, 474.

21 M. J. L. Gines and E. Iglesia, *J. Catal.*, 1998, **176**, 155.

22 C. Gardner Swain, A. L. Powell, W. A. Sheppard and C. R. Morgan, *J. Am. Chem. Soc.*, 1979, **101**(13), 3576.

23 H. Berberich and P. W. Roesky, *Angew. Chem., Int. Ed.*, 1998, **37**(11), 1569.

This journal is © The Royal Society of Chemistry 2017

24 (*a*) G. Kresse and J. Furthmuller, *Comput. Mater. Sci.*, 1996, **6**, 15; (*b*) J. Perdew, *Phys. Rev. B: Condens. Matter Mater. Phys.*, 1992, **46**, 6671; (*c*) D. Vanderbilt, *Phys. Rev. B: Condens. Matter Mater. Phys.*, 1990, **41**, 7892; (*d*) G. Mills, H. Jonsson and G. K. Schenter, *Surf. Sci.*, 1995, **324**, 305; (*e*) H. Jónsson, G. Mills and K. W. Jacobsen, in *Classical and quantum dynamics in condensed phase simulations*, World Scientific, Singapore, 1998; (*f*) G. Henkelman, B. P. Uberuaga and H. J. Jonsson, *J. Chem. Phys.*, 2000, **113**, 9901; (*g*) G. Henkelman and H. Jonsson, *J. Chem. Phys.*, 2000, **113**, 9978; (*h*) G. Henkelman and H. Jonsson, *J. Chem. Phys.*, 1999, **111**, 7010; (*i*) X. Qian, J. Li, L. Qi, C. Wang, T. Chan, Y. Yao, K. Ho and S. Yip, *Phys. Rev. B: Condens. Matter Mater. Phys.*, 2008, **78**, 245112.

25 S. M. Johnston, A. Mulligan, V. Dhanak and M. Kadodwala, *Surf. Sci.*, 2004, **548**, 5.

26 C. L. A. Lamont, W. Stenzel, H. Conrad and A. M. Bradshaw, *J. Electron Spectrosc. Relat. Phenom.*, 1993, **64**, 287.

27 Y. Ishikawa, M. Liao and R. C. Cabrera, *Surf. Sci.*, 2000, **463**, 66.

28 J. R. B. Gomes, J. Gomes and F. Illas, *J. Mol. Catal. A: Chem.*, 2001, **170**, 187.

29 S. K. Desai, M. Neurock and K. Kourtakis, *J. Phys. Chem. B*, 2002, **106**, 2559.

30 R. I. Masel, *Principles of Adsorption and Reaction on Solid Surfaces*, J. Wiley and Sons, New York, 1996.

31 N. K. Sinha and M. Neurock, *J. Catal.*, 2012, **295**, 31.

32 D. Cao, G. Q. Lu, A. Wieckowski, S. Wasileski and M. Neurock, *J. Phys. Chem. B*, 2005, **109**, 11622.

33 S. K. Desai and M. Neurock, *Phys. Rev. B: Condens. Matter Mater. Phys.*, 2003, **68**, 075420.

34 S. K. Desai, V. Pallassana and M. Neurock, *J. Phys. Chem. B*, 2001, **105**, 9171.

35 C. Ammon, A. Bayer, G. Held, B. Richer, T. Schmidt and H. P. Steinrück, *Surf. Sci.*, 2002, **507**, 845.

36 M. Bowker and R. J. Madix, *Surf. Sci.*, 1980, **95**, 190.

37 M. Bowker and R. J. Madix, *Surf. Sci.*, 1982, **116**, 549.

38 P. D. A. Pudney, S. A. Francis, R. W. Joyner and M. Bowker, *J. Catal.*, 1991, **131**, 104.

39 B. N. Zope, D. D. Hibbitts, M. Neurock and R. J. Davis, *Science*, 2010, **330**, 74.

40 D. Hibbitts and M. Neurock, *Surf. Sci.*, 2016, **650**, 210.

41 D. Hibbitts and M. Neurock, *J. Catal.*, 2013, **299**, 261.

42 W. B. Jensen, *The Lewis acid–base concepts: An overview*, J. Wiley, 1979.

43 F. Calaza, D. Stacchiola, M. Neurock and W. T. Tysoe, *J. Am. Chem. Soc.*, 2010, **132**(7), 2202.

44 D. Stacchiola, F. Calaza, L. Burkholder, A. W. Schwabacher, M. Neurock and W. T. Tysoe, *Angew. Chem., Int. Ed.*, 2005, **44**(29), 4572.

45 R. J. Madix and J. T. Roberts, in *Surface Reactions*, ed. R. J. Madix, Springer-Verlag, Berlin, 1994, p. 5.

46 Q. Xing, W. Pei and *et al.*, *Fundamental Organic Chemistry*, Higher Education Press, China, 2005.

47 T. Akashi, S. Sato and K. Inui, *Catal. Commun.*, 2002, **4**, 411.

48 D. J. Elliot and F. J. Pennella, *J. Catal.*, 1989, **119**, 359.

49 B. Xu, X. Liu, J. Haubrich, R. J. Madix and C. M. Friend, *Angew. Chem., Int. Ed.*, 2009, **48**, 4206.

50 B. Xu, J. Haubrich, T. A. Baker, E. Kaxiras and C. M. Friend, *J. Phys. Chem. C*, 2011, **115**, 3703.

51 X. Liu, B. Xu, J. Haubrich, R. J. Madix and C. M. Friend, *J. Am. Chem. Soc.*, 2009, **131**, 5757.

52 R. A. van Santen and M. Neurock, *Molecular Heterogeneous Catalysis: A Mechanistic and Computational Approach*, VCH-Wiley, Inc., 2006.

53 S. C. Luo and J. L. Falconer, *Catal. Lett.*, 1999, **57**, 89.

54 J. E. Rekoske and M. A. Barteau, *Ind. Eng. Chem. Res.*, 2011, **50**, 41.

55 V. V. Ordomsky, V. L. Sushkevich and I. Ivanova, *J. Mol. Catal. A: Chem.*, 2010, **333**, 85.

56 J. M. Sun, K. K. Zhu, F. Gao, C. M. Wang, J. Liu, C. H. F. Peden and Y. Wang, *J. Am. Chem. Soc.*, 2011, **133**, 11096.

57 K. Tanabe and T. Yamaguchi, *Catal. Today*, 1994, **20**, 185.

58 K. Tanabe and W. F. Holderich, *Appl. Catal., A*, 1999, **181**, 399.

59 K. Tanabe, *Appl. Catal., A*, 1994, **113**, 147.